Variable Impedance Control of Redundant Manipulators for Intuitive Human–Robot Physical Interaction

Fanny Ficuciello, *Member, IEEE*, Luigi Villani, *Senior Member, IEEE*, and Bruno Siciliano, *Fellow, IEEE*

***Abstract*—This paper presents an experimental study on human–robot comanipulation in the presence of kinematic redundancy. The objective of the work is to enhance the performance during human–robot physical interaction by combining Cartesian impedance modulation and redundancy resolution. Cartesian impedance control is employed to achieve a compliant behavior of the robot's end effector in response to forces exerted by the human operator. Different impedance modulation strategies, which take into account the human's behavior during the interaction, are selected with the support of a simulation study and then experimentally tested on a 7-degree-of-freedom KUKA LWR4. A comparative study to establish the most effective redundancy resolution strategy has been made by evaluating different solutions compatible with the considered task. The experiments have shown that the redundancy, when used to ensure a decoupled apparent inertia at the end effector, allows enlarging the stability region in the impedance parameters space and improving the performance. On the other hand, the variable impedance with a suitable modulation strategy for parameters' tuning outperforms the constant impedance, in the sense that it enhances the comfort perceived by humans during manual guidance and allows reaching a favorable compromise between accuracy and execution time.**

***Index Terms*—Force control, physical human–robot interaction, redundant robots.**

I. Introduction

In the face of the unpredictability of human behaviors, the adoption of suitable impedance strategies [1], [2] to control robots in the presence of humans is an essential paradigm to ensure reliability and safety. For advanced robots, which operate in anthropic environments by cooperating with humans and substituting them in some tasks, the quality of performance is not just about accuracy and repeatability. Indeed, it rather depends on the ability of the robots to adapt their behaviors dynamically and according to the task and human intentions. In the case of redundant robots, also the redundant degrees of freedom (DOFs) may play an important role both in the stability of the coupled system and in the quality of performance.

This paper presents an experimental study on a variable impedance control of a redundant manipulator not specifically designed for human–robot cooperation, used for the execution of a task under human guidance. In particular, a cooperative writing task is used as case study, and a Cartesian impedance control law is adopted to achieve a compliant behavior of the end effector with respect to the forces exerted by the human operator.

The main idea of the paper is that of using in a synergic way the robot's redundancy and the modulation of the Cartesian impedance parameters to enhance the performance during human–robot physical interaction. In particular, an experimental evaluation of different impedance modulation laws within a stability region is carried out, while it is shown that the overall performance can be improved when the redundancy is used to enlarge the stability region in the space of the impedance parameters.

Considering that instability is likely to occur during interaction when the controller attempts to impose to the robot an impedance behavior, which is significantly different from the intrinsic hardware dynamics, in a recent paper [3], we have proposed to exploit redundancy to make the robot equivalent inertia at the end effector as close as possible to the desired inertia. In particular, since comanipulation tasks typically require a decoupled impedance along the Cartesian directions, the redundant DOFs are used to reduce as much as possible the dynamic coupling of the end effector equivalent inertia.

The preliminary results presented in [3] are extended here through an extensive experimental study to establish the most advantageous solution for the use of redundancy. In detail, it is shown that robot's redundancy, when used to ensure a decoupled apparent inertia at the end effector, allows enlarging the stability region in the impedance parameters space and improves the performance.

On the other side, different modulation strategies for the impedance parameters are proposed and tested. The parameters are modulated online during the interaction according to the human's behavior, which is inferred through the measurements of the end effector velocities. The solution adopted for our robotic platform consists on linking the parameters variation directly to the Cartesian velocity. This approach has been validated by means of a preliminary simulation study and tested experimentally.

Manuscript received December 31, 2014; revised March 8, 2015; accepted April 30, 2015. Date of publication May 20, 2015; date of current version August 4, 2015. This paper was recommended for publication by Associate Editor V. Kyrki and Editor A. Kheddar upon evaluation of the reviewers' comments. This work was supported in part by the EC Seventh Framework Programme (FP7) within SAPHARI project 287513 and RoDyMan project 320992.

The authors are with the Dipartimento di Ingegneria Elettrica e Tecnologie dell'Informazione, Università degli Studi di Napoli Federico II, 80125 Napoli, Italy (e-mail: fanny.ficuciello@unina.it; luigi.villani@unina.it; bruno.siciliano@unina.it).

This paper has supplementary downloadable material available at http://ieeexplore.ieee.org.

Color versions of one or more of the figures in this paper are available online at http://ieeexplore.ieee.org.

Digital Object Identifier 10.1109/TRO.2015.2430053

1552-3098 © 2015 IEEE. Personal use is permitted, but republication/redistribution requires IEEE permission.
See http://www.ieee.org/publications_standards/publications/rights/index.html for more information.

The experimental results show that the variable impedance control performs better than the impedance control with constant parameters, in the sense that it preserves accuracy while reducing the execution time, in comparison with high constant impedance, and it guarantees a good execution speed with increased accuracy, in comparison with low constant impedance. Finally, the use of the variable impedance strategy together with Cartesian inertia decoupling through redundancy resolution is the combination that allows the best performance and effectively enhances the comfort level perceived by the human operators during manual guidance. In our knowledge, this is the first paper where variable impedance and redundancy resolution are used in a combined way to improve stability and performance during human guidance.

This paper is organized as follows. Section II describes research work related to impedance modulation strategies and stability issues in human–robot interaction. In Section III, the Cartesian impedance control of redundant robots is briefly summarized, while the possible criteria for redundancy resolution are presented in Section IV. Section V presents the experimental study that has been performed to estimate the stability region in the impedance parameter space. In Section VI, the rules for the selection of the impedance parameters are discussed. The experimental evaluation of the different options for redundancy resolution as well as for the selection of the impedance modulation laws is presented in Section VII. Finally, a discussion of the results and the conclusion is drawn in Sections VIII and IX, respectively.

II. Related Works

In recent years, the research effort on finding appropriate impedance control strategies for human–robot physical interaction is going toward learning and imitation of impedance modulation strategies of living beings.

A possible solution is represented by variable impedance actuators (VIAs) using different technologies to create a new generation of robots that can regulate their impedance behavior in a controlled way [4].

For robot manipulators not using VIAs, a number of adaptive impedance/admittance strategies have been proposed for human–robot collaborative tasks, where the control gains are tuned on the basis of the inferred human intentions. Several studies propose modulation strategies based on the estimation of the human impedance computed using the forces and the positions measured during the task execution. In [5] and [6], the variation of the impedance parameters is determined on the basis of the data collected from experiments where a robot and a human execute the cooperative task. In [5], a simple switching strategy between preselected values is implemented, while in [6], an optimal value for the damping, which minimizes a suitable cost function, is computed online.

The estimation of the human operator's arm impedance is not easy, and some simplifications may occur. For example, at low velocities, the stiffness is usually computed assuming that it is the dominant impedance feature [7], [8]. More accurate measurements methods of human impedance have been adopted by neuroscientists to analyze human movement control [9] and, in particular, the strategy used by the human central nervous system to deal with instability [10]. Inspired to these studies, a learning control technique is proposed in [11] to optimally adapt robot's impedance during the interaction with dynamic environments and humans. Learning techniques have been adopted also to extract and transfer impedance modulation strategies from humans to variable impedance robots [12] or, complementary, to teach variable stiffness tasks to robots through physical interaction with a human operator [13].

A further method to transfer human skills in impedance regulation to robots interacting with uncertain environments is based on the concept of teleimpedance [14]. In this case, a suitable human–machine interface allows us to provide the slave robot with a position reference and an end-point stiffness reference; this latter is estimated in real time from the measured electromyogram signals of eight muscles of the arm of the human master.

In the applications where the robot must be free to move under the forces applied by humans, the desired stiffness is usually set to zero, as well as the desired position, while the damping and mass parameters can be tuned, for example, depending on the velocity and acceleration of the human operator [15]. On the other hand, in surgical and rehabilitation scenarios, stiffness regulation plays an important role to ensure accuracy and safety in the presence of both preplanned target and interaction with unpredictable dynamic environments. An interesting method that allows us to reproduce a specific time-varying stiffness profile during needle insertion by preserving passivity is proposed in [16], while the implementation of safe constraints along a specific task or to limit the user to stay within a safe region is considered in [17]. These topics are also of interest in the applications where collaborative robots (Cobots) are employed [18].

For variable impedance control, a crucial issue is that stability must be guaranteed for all the possible range of variation of the parameters. The stability depends on how impedance control is implemented (e.g., with or without force measurements, or whether an impedance or an admittance law is used), but also on the robot's hardware; namely, the robot kinematics and dynamics, the kind of transmission, the presence of friction and of structural compliance, the kind of sensors and actuators [15], [19]. Moreover, the overall coupled dynamics of the robot and human must be considered [20].

Stability of impedance control has been investigated in the seminal works of Hogan [1] and later on in [21], using the concept of passivity, and in [22], where the natural admittance control is introduced. Admittance and impedance are defined in a reciprocal way: Impedance control produces forces/torques in response to velocities, while admittance control produces velocities in response to forces and torques.

When the robot is driven by the human, a low robot impedance is typically required. In particular, the stiffness should be low and often null, while damping should be decreased when fast movements without particular accuracy are required and increased to perform fine motions. On the other hand, the apparent inertia of the robot cannot be arbitrarily decreased because the stability can be lost.

Often, the structural impedance of common robots, including lightweight robots like the KUKA LWR4 arm considered

in this paper, is higher than the ideal impedance required for an effective cooperation with humans. In particular, the equivalent inertia of the robot at the contact point (which hereafter is assumed to be the end effector) may be too high and must be reduced. This can be done by using feedback of the exchanged force.

In this respect, using a simple 1-DOF model, it has been theoretically proven that, by reducing the inertia more than a given threshold below its physical value, the system loses passivity [21], due to the presence of unavoidable structural compliance between the actuators and the interaction force. The passivity property is a sufficient condition that guarantees coupled stability in the presence of interaction with a generic passive environment. This threshold holds also for natural admittance control [22] which, with respect to impedance control, allows reducing the effects of friction and unmodeled disturbances, independently of inertia. On the other hand, theoretical and experimental studies have shown that passivity may be too conservative and can be relaxed to improve performance [20], [23], [24].

III. Cartesian Impedance Control

The KUKA LWR4 arm is a 7-DOF robot that can be torque or velocity controlled; therefore, both impedance and admittance control can be used. The two control approaches have complementary pros and cons, which have been well documented in the literature (see, e.g., [25]). In this study, impedance control is considered.

The dynamic model of the robot has the form

$$\boldsymbol{M}(\boldsymbol{q})\ddot{\boldsymbol{q}} + \boldsymbol{C}(\boldsymbol{q},\dot{\boldsymbol{q}})\dot{\boldsymbol{q}} + \boldsymbol{g}(\boldsymbol{q}) + \boldsymbol{\tau}_f = \boldsymbol{\tau}_c + \boldsymbol{J}^T(\boldsymbol{q})\boldsymbol{F}_{\text{ext}} \quad (1)$$

where $\boldsymbol{q} \in \mathbb{R}^n$, with $n = 7$, is the vector of joint variables, $\boldsymbol{M}(\boldsymbol{q})$ is the inertia matrix, $\boldsymbol{C}(\boldsymbol{q},\dot{\boldsymbol{q}})\dot{\boldsymbol{q}}$ is the vector of Coriolis/centrifugal torques, $\boldsymbol{g}(\boldsymbol{q})$ is the vector of gravitational torques, $\boldsymbol{\tau}_f$ is the vector of the friction torques, $\boldsymbol{\tau}_c$ is the control torque, $\boldsymbol{J}(\boldsymbol{q})$ is the robot Jacobian, and $\boldsymbol{\tau}_{\text{ext}} = \boldsymbol{J}^T\boldsymbol{F}_{\text{ext}}$ is the joint torque resulting from external force and torque $\boldsymbol{F}_{\text{ext}}$ applied to the end effector.

The control strategy is designed to perform tasks in cooperation with humans. The operator interacts with the robot by moving the end effector along arbitrary trajectories. It is assumed that only forces can be applied. Hence, in (1), $\boldsymbol{F}_{\text{ext}}$ is the (3×1) vector of external forces and $\boldsymbol{J}(\boldsymbol{q})$ is the (3×7) Jacobian relating the joint velocities to the end effector translational velocity.

To design the impedance control, it is useful to derive the end effector dynamics in the operational space [26], considering only the translational motion

$$\boldsymbol{\Lambda}(\boldsymbol{q})\ddot{\boldsymbol{x}} + \boldsymbol{\mu}(\boldsymbol{q},\dot{\boldsymbol{q}})\dot{\boldsymbol{x}} + \boldsymbol{F}_g(\boldsymbol{q}) + \boldsymbol{F}_f(\boldsymbol{q}) = \boldsymbol{F}_c + \boldsymbol{F}_{\text{ext}} \quad (2)$$

where $\boldsymbol{x} \in \mathbb{R}^3$ is the Cartesian position vector of the end effector, $\boldsymbol{\Lambda} = (\boldsymbol{J}\boldsymbol{M}^{-1}\boldsymbol{J}^T)^{-1}$ is the (3×3) end effector inertia matrix, hereafter denoted as apparent inertia, while $\boldsymbol{\mu}\dot{\boldsymbol{x}} = \boldsymbol{\Lambda}(\boldsymbol{J}\boldsymbol{M}^{-1}\boldsymbol{C} - \dot{\boldsymbol{J}})\dot{\boldsymbol{q}}$, $\boldsymbol{F}_g = \boldsymbol{J}^{\dagger T}\boldsymbol{g}$, $\boldsymbol{F}_f = \boldsymbol{J}^{\dagger T}\boldsymbol{\tau}_f$ and $\boldsymbol{F}_c = \boldsymbol{J}^{\dagger T}\boldsymbol{\tau}_c$ are the forces, reflected at the end effector, corresponding to the noninertial joint torques in (1).

Equation (2) describes only the end effector dynamics and does not include the so-called null space dynamics. Matrix $\boldsymbol{J}^\dagger$ is the dynamically consistent generalized inverse of matrix $\boldsymbol{J}$, defined as [26]

$$\boldsymbol{J}^\dagger = \boldsymbol{M}^{-1}\boldsymbol{J}^T[\boldsymbol{J}\boldsymbol{M}^{-1}\boldsymbol{J}^T]^{-1}. \quad (3)$$

It can be proven that, only with this choice of generalized inverse, the null-space dynamics does not affect the end effector behavior. Moreover, when the Jacobian is close to a singularity, the generalized inverse can be robustly approximated using the damped least squares pseudoinverse [27].

In order to make the end effector able to follow and adapt to the force exerted by the operator at the tip, the end effector dynamics can be set as a mass–damper system of

$$\boldsymbol{\Lambda}_d\ddot{\boldsymbol{x}} + \boldsymbol{D}_d\dot{\boldsymbol{x}} = \boldsymbol{F}_{\text{ext}} \quad (4)$$

where $\boldsymbol{\Lambda}_d$ and $\boldsymbol{D}_d$ are suitable inertia and damping matrices, which are positive definite and are usually set as constant diagonal matrices.

The above dynamics can be imposed to the closed loop controlled system by choosing $\boldsymbol{F}_c$ in (2) as

$$\boldsymbol{F}_c = \boldsymbol{\eta}(\boldsymbol{q},\dot{\boldsymbol{q}}) - \boldsymbol{\Lambda}(\boldsymbol{q})\boldsymbol{\Lambda}_d^{-1}\boldsymbol{D}_d\dot{\boldsymbol{x}} + (\boldsymbol{\Lambda}(\boldsymbol{q})\boldsymbol{\Lambda}_d^{-1} - \boldsymbol{I})\boldsymbol{F}_{\text{ext}} \quad (5)$$

with $\boldsymbol{\eta}(\boldsymbol{q},\dot{\boldsymbol{q}}) = \boldsymbol{\mu}(\boldsymbol{q},\dot{\boldsymbol{q}})\dot{\boldsymbol{x}} + \boldsymbol{F}_g(\boldsymbol{q}) + \boldsymbol{F}_f(\boldsymbol{q})$.

This equation is a Cartesian impedance control law with null stiffness and null virtual position. If the apparent inertia of the end effector is left unchanged, i.e., $\boldsymbol{\Lambda}_d = \boldsymbol{\Lambda}(\boldsymbol{q})$, the control law (5) does not depend on the external force $\boldsymbol{F}_{\text{ext}}$. Conversely, force feedback is required if inertia reshaping is desired. This is the price to pay to achieve the ideal behavior described by (4), which is linear, decoupled, and independent of the robot configuration. On the other hand, if the natural inertia is preserved, a configuration-dependent damping matrix should be adopted to guarantee stability (see, e.g., [28]) leading to a nonlinear, coupled, and configuration-dependent dynamics, which would make more difficult for the user to lead the end effector.

The external force can be measured by using a force/torque sensor mounted at the end effector. Alternatively, force estimation techniques can be adopted. An effective method, introduced in [29], is based on the generalized momentum $\boldsymbol{p}(t) = \boldsymbol{M}(\boldsymbol{q})\dot{\boldsymbol{q}}$ and the n-dimensional residual vector $\boldsymbol{r}$ defined as

$$\boldsymbol{r}(t) = \boldsymbol{K}_I\left[\int_0^t (\boldsymbol{\tau}_c - \boldsymbol{g}(\boldsymbol{q}) + \boldsymbol{r}(\sigma))d\sigma - \boldsymbol{p}(t)\right] \quad (6)$$

with $\boldsymbol{r}(0) = \boldsymbol{0}$ and $\boldsymbol{K}_I$ a diagonal positive matrix. These quantities can be computed using measured signals $\boldsymbol{q}$, $\dot{\boldsymbol{q}}$ and the control torque $\boldsymbol{\tau}_c$. It can be shown that

$$\boldsymbol{r} \approx \boldsymbol{\tau}_{\text{ext}} - \boldsymbol{\tau}_\delta \quad (7)$$

with $\boldsymbol{\tau}_\delta = \boldsymbol{C}(\boldsymbol{q},\dot{\boldsymbol{q}})\dot{\boldsymbol{q}} + \boldsymbol{\tau}_f$. Hence, left multiplying both sides of the above equation by $\boldsymbol{J}^{\dagger T}$ yields

$$\boldsymbol{J}^{\dagger T}\boldsymbol{r} \approx \boldsymbol{J}^{\dagger T}\boldsymbol{\tau}_{\text{ext}} - \boldsymbol{J}^{\dagger T}\boldsymbol{\tau}_\delta \approx \boldsymbol{F}_{\text{ext}}$$

where the contribution of friction torques and Coriolis and centrifugal effects reflected at the end effector has been considered negligible with respect to the external force. Therefore, vector

$$\widehat{\boldsymbol{F}}_{\text{ext}} = \boldsymbol{J}^{\dagger T}\boldsymbol{r} \quad (8)$$

is an estimate of the external force.

In view of the above approximations, the control law that imposes the impedance dynamics (4) can be implemented in the joint space in the form

$$\boldsymbol{\tau}_{\mathrm{imp}} = -\boldsymbol{J}^T \boldsymbol{\Lambda}[\dot{\boldsymbol{J}}\dot{\boldsymbol{q}} + \boldsymbol{\Lambda}_d^{-1}(\boldsymbol{D}_d\dot{\boldsymbol{x}} - \widehat{\boldsymbol{F}}_{\mathrm{ext}})] + \boldsymbol{g}(\boldsymbol{q}) - \boldsymbol{r}. \quad (9)$$

IV. Redundancy Resolution

In the presence of redundant DOFs, which is the case considered here, it is possible to assign a secondary task in the null space of the end effector task, by using the control law [26]

$$\boldsymbol{\tau}_c = \boldsymbol{\tau}_{\mathrm{imp}} + (\boldsymbol{I} - \boldsymbol{J}^T\boldsymbol{J}^{\dagger T})(\boldsymbol{u} - k_D\dot{\boldsymbol{q}}) \quad (10)$$

where $-k_D\dot{\boldsymbol{q}}$, with $k_D > 0$, is a suitable damping torque, and $\boldsymbol{u}$ is a torque control input to be designed, corresponding to a secondary task, which is projected in the null space of the main task through the matrix $\boldsymbol{I} - \boldsymbol{J}^T\boldsymbol{J}^{\dagger T}$.

As observed in [30], control law (10) is able to ensure stability in practice both for the end effector task and in the null space. A rigorous stability proof would require a more complex formulation of the null space terms, as those presented in [31] and [32] and generalized in [33] to the case of an arbitrary hierarchy of null space tasks.

In our application, the human guidance of the end effector involves only the position, which is made compliant by the Cartesian impedance control under the action of the external forces. Thus, there are four of the seven DOFs of the robot at disposal for the secondary task.

Moreover, in the task considered in this paper, i.e., writing on a planar surface, the pen should point always toward the surface. For this reason, among the possible redundancy resolution criteria, we have selected those that are less influenced by the end effector orientation, at least in region of the workspace where the main task is executed. This feature was also verified experimentally. Another possibility would have been that of controlling also the orientation to a desired value, or to make the end effector compliant under the action of the external torques. In this case, however, a robot with a large number of DOFs (larger than 7) would be required to usefully exploit the redundancy.

Different criteria can be pursued in order to choose the secondary task.

One simple criterion can be that of keeping the robot as far as possible from kinematic singularities. This can be achieved, e.g., by maximizing the kinematic manipulability index, defined as

$$m(\boldsymbol{q}) = \sqrt{\det(\boldsymbol{J}\boldsymbol{J}^T)} \quad (11)$$

i.e., by choosing $\boldsymbol{u}$ in (10) as

$$\boldsymbol{u} = k_m \left(\frac{\partial m(\boldsymbol{q})}{\partial \boldsymbol{q}}\right)^T \quad (12)$$

where the elements of the gradient of the manipulability index can be computed as [34]

$$\frac{\partial m(\boldsymbol{q})}{\partial q_i} = m(\boldsymbol{q})\mathrm{trace}\left[\frac{\partial \boldsymbol{J}}{\partial q_i}\boldsymbol{J}^{\dagger}\right]. \quad (13)$$

Notice that the manipulability index is proportional to the area of the velocity manipulability ellipsoid, which represents the capability of the robot to move the end effector along the Cartesian directions, with a given set of unit norm joints velocities. Hence, in a joint configuration where this index is (locally) maximized, it is possible to produce end effector velocities in all possible directions with (locally) minimal joint velocities.

In theory, instead of trying to make the ellipsoid as similar as possible to a sphere, it could be useful to shape it so that the principal axis are always suitably aligned to the significant directions of the task. However, the continuous changes of direction imposed by the human to the end effector may produce continuous internal motions of the robot that can have undesired effects (e.g., collisions or fast reconfigurations that are unsafe for the human operator). Therefore, this solution, after some tests, was discarded.

Another possibility of exploiting redundancy is that of trying to optimize in some way the mapping between the forces applied to the end effector and the corresponding velocities or accelerations. As a matter of fact, in ideal conditions, the Cartesian impedance control law (5) allows cancelling out the robot dynamics as well as making the end effector dynamics completely independent of the joint configuration. On the other hand, it has been proven both theoretically and experimentally that, during interaction, instability is likely to occur when the controller attempts to impose to the robot a dynamic behavior that differs significantly from the intrinsic hardware dynamics (in particular, lower than the natural robot impedance). Hence, the idea pursued here is that of using redundancy to make the robot apparent dynamics at the end effector, described by (2), as close as possible to the desired dynamics (4).

The most critical element in (2) is the equivalent inertia, which is configuration dependent. This means that, at any given end effector position, the internal motion allowed by redundancy could be exploited to achieve robot's configurations with desired inertial properties. Of course, this can be done only within certain limits, depending on the robot kinematic structure and on the mass distribution. What it is reasonable, for example, is to choose joint configurations with maximally decoupled inertia. As in [3], this is achieved by using a secondary task function inspired to the dynamic conditioning index (DCI) introduced in [35] to measure the dynamic isotropy of robot manipulators in joint space.

In the Cartesian space, the DC index (DCI) can be defined as the least-squares difference between the generalized inertia matrix and a diagonal matrix as

$$\omega(\boldsymbol{q}) = \frac{1}{2}\boldsymbol{E}^T(\boldsymbol{q})\boldsymbol{W}\boldsymbol{E}(\boldsymbol{q}) \quad (14)$$

where $\boldsymbol{W}$ is a diagonal weighting matrix, and the error vector $\boldsymbol{E}(\boldsymbol{q})$ is defined as

$$\boldsymbol{E}(\boldsymbol{q}) = \begin{bmatrix} \lambda_{11}(\boldsymbol{q}) - \sigma(\boldsymbol{q}) \\ \lambda_{22}(\boldsymbol{q}) - \sigma(\boldsymbol{q}) \\ \lambda_{33}(\boldsymbol{q}) - \sigma(\boldsymbol{q}) \\ \lambda_{12}(\boldsymbol{q}) \\ \lambda_{13}(\boldsymbol{q}) \\ \lambda_{23}(\boldsymbol{q}) \end{bmatrix} \quad (15)$$

with being λ_{ij} the generic element of the inertia matrix $\boldsymbol{\Lambda}$ and σ defined as

$$\sigma(\boldsymbol{q}) = \frac{1}{3}\text{trace}(\boldsymbol{\Lambda}(\mathbf{q})). \tag{16}$$

The minimization of $\omega(\boldsymbol{q})$ results in a minimization of the elements' norm of $\boldsymbol{E}$, which corresponds to (a local) maximally diagonal inertia.

The weighting matrix $\boldsymbol{W}$ has been chosen in order to give priority to the minimization of the norm of the off-diagonal elements of $\boldsymbol{\Lambda}(\boldsymbol{q})$, e.g.,

$$\boldsymbol{W} = \text{diag}\{\boldsymbol{I}_3, \mu \boldsymbol{I}_3\} \tag{17}$$

with $\mu > 1$ and $\boldsymbol{I}_3$ denoting the (3×3) identity matrix.

Finally, the control input $\boldsymbol{u}$ in (14) is chosen as

$$\boldsymbol{u} = -k_c \left(\frac{\partial \omega(\boldsymbol{q})}{\partial \boldsymbol{q}}\right)^T \tag{18}$$

with $k_c > 0$.

V. Stability Region

A suitable procedure has been set up to find the allowed range of variation of the impedance parameters of (4) so that stability is preserved.

The stability region in the impedance parameters space could be estimated analytically (see, e.g., [24]). However, many authors have observed that the actual bounds of the stability region are dependent on the robot's hardware and, in the case of interaction with a human operator, also on the impedance of the human arm, which cannot be accurately modeled and evaluated [19], [20]. A further complication here is represented by the null-space stability for the presence of redundant DOFs [30]. Therefore, in this study, the stability region has been found experimentally.

In the scalar case, (4) can be rewritten in the Laplace domain as

$$V(s) = \frac{1}{D}\frac{1}{1+sT}F(s) \tag{19}$$

where V and F are the Laplace transforms of the velocity and force, respectively, and $T = \lambda/D$ is the time constant of the system, where λ and D represent the inertia and damping along a generic Cartesian direction, respectively. Hence, it can be argued that the lower the damping, the higher the steady-state velocity for a given constant input force; moreover, for a given damping, the lower the inertia, the higher the bandwidth of the system or, equivalently, the lower the time constant T.

For the stability test, the joint vector

$$\boldsymbol{q}_0 = [0 \quad 0 \quad 0 \quad -90 \quad 0 \quad -45 \quad 0]^T$$

corresponding to the robot configuration represented in Fig. 1, has been selected. One reason for this choice is that, in this configuration, the end effector inertia matrix is almost diagonal. Another reason is that, in this configuration, one of the eigenvalues of the inertia matrix (that corresponding to the vertical axis) assumes a value $\bar{\lambda}$ close to the maximum one, in the portion of the robot workspace where the task is executed. Hence, $\boldsymbol{q}_0$ is a worst-case configuration for scaling (reducing) the end effector inertia.

Fig. 1. Robot KUKA LWR4 in the configuration chosen for stability evaluation.

Indeed, if a desired isotropic Cartesian inertia is imposed, the dynamics along the vertical direction is the most critical for stability, being the direction where the ratio between the desired and actual mass is the lowest, also in a neighborhood of the joint configuration $\boldsymbol{q}_0$. This means that the stability bounds for the parameters along the vertical direction are the most conservative and ensure stability also along the other directions, as well as in the surrounding configurations.

The value of the inertia matrix in $\boldsymbol{q}_0$ and the corresponding vector of eigenvalues are

$$\boldsymbol{\Lambda}(\boldsymbol{q}_0) = \begin{bmatrix} 0.1187 & 0.0006 & 0.0226 \\ 0.0006 & 0.3069 & -0.1395 \\ 0.0226 & -0.1395 & 4.2405 \end{bmatrix}$$

$$\boldsymbol{\lambda}(\boldsymbol{q}_0) = [0.1186 \quad 0.3020 \quad 4.2456]^T.$$

To reduce the number of parameters, the same damping and the same mass has been set along all the directions of the Cartesian space, i.e., $\boldsymbol{D}_d = D\boldsymbol{I}$ and $\boldsymbol{\Lambda}_d = \lambda \boldsymbol{I}$, with $\lambda = \alpha\bar{\lambda}$, being $\bar{\lambda} = 4.2456$ kg the maximum eigenvalue and $0 < \alpha \leq 1$ a scaling factor. This way, the desired impedance behavior will be made isotropic by decreasing the mass along the vertical direction and increasing those along the other two Cartesian directions, which, therefore, are not critical for stability.

The stability region has been evaluated experimentally by setting a value of damping D in the interval $[5, 60]$ Ns/m and reducing the value of α, starting from $\alpha = 1$, until vibrations can be felt by an operator shaking the end effector in a neighborhood of the initial configuration. In order to have results independent of the stiffness of the specific subject, the end effector is shaken so as to produce large variations of the stiffness of the

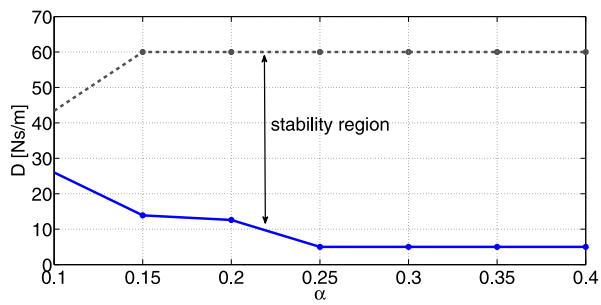

Fig. 2. Range of minimum and maximum allowed damping D for a given scaling factor α of the inertia matrix.

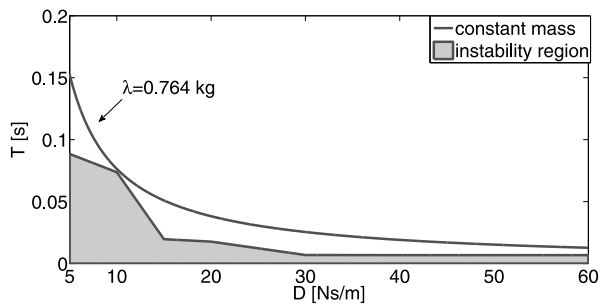

Fig. 3. Stability region: time constant T versus damping D.

human arm. The amplitude of the interval for the damping coefficient has been set on the basis of experiments where the natural robot's inertia was not modified.

The results of the experimental procedure are reported in Fig. 2, where the stability region for the parameters D and α is that included between the continuous and the dotted line. It can be observed that any value of damping in the interval $[5, 60]$ can be chosen provided that $\alpha > 0.25$, while, for $\alpha < 0.25$ the lower and upper bounds of the allowed damping come closer. For $\alpha < 0.1$, the robot starts vibrating for any value of damping.

An alternative representation is reported in Fig. 3, where the stability region is parameterized with respect to the time constant T of the impedance (19) and to the damping D. In this figure, also the geometric locus with minimum constant mass ($\lambda = 0.764$ kg) contained in the stability region is represented. This curve can be taken as a rough analytic expression of the frontier of the stability region, i.e., stability is preserved for any choice of the impedance parameters in the region on the right of this curve.

It is worth observing that, since the end effector dynamics is not homogenous along the three Cartesian directions, it would be significant to choose different impedance parameters along these directions. Therefore, a different stability region in the parameters space could be defined for each Cartesian direction. Actually, the three stability regions have been found experimentally (see Fig. 9), using the same procedure described above, and will be used in Section VII.

VI. Variable Impedance

The goal of a variable impedance strategy for a comanipulation task is to vary the damping and mass properties of the robot in order to accommodate the human movement during physical interaction. According to the related results available in the literature [6], [15], [19], high impedance parameters are desired when the operator performs fine movements at low velocity, while lower values of the parameters should be used for large movements at high velocity. The human perception is mainly influenced by the damping parameter, while, for a given damping, the desired (virtual) mass is crucial for stability.

Therefore, our idea is that of varying the damping according to the absolute value of the end effector Cartesian velocity in order to improve the performance in terms of execution time and accuracy. Namely, when the velocity is high, the damping force is reduced so that the operator can move the end effector with minimum effort and the execution time can be reduced; vice versa, at low velocity, the damping force is increased to improve accuracy. On the other hand, the virtual mass is set so as the parameters of the system remain in the stability region. To this purpose, the stability region in the parameter space has been evaluated experimentally (see Section V) for any damping in the interval $[5, 60]$ N · s/m.

The relationships used to vary the damping for each of the Cartesian principal directions is

$$D(\dot{x}) = \min\{a\,\mathrm{e}^{-b|\dot{x}|}, 5\} \tag{20}$$

where $a = 60$ and $b = 4$. These parameters have been chosen in order to have a variation of the damping within the interval $[5, 60]$ N · s/m for the possible range of velocities in the considered task. A saturation to the minimum value of 5 N · s/m is introduced in case of high velocity.

For the mass (or, equivalently, for the time constant T), different choices have been considered and tested, namely:

- L1: constant mass, with low value (close to the minimum value within the stability region), i.e. $\lambda = 1.1$ kg.
- L2: constant mass, with high value, i.e. $\lambda = 5.6$ kg.
- L3: constant T, set as the minimum value within the stability region for any damping D.
- L4: minimum (variable) T within the stability region for any damping D.

In the latter case, the time constant T is computed as

$$T = \frac{\lambda_f}{D_f}(a + b\arctan(c(D - d)))$$

where the default damping value $D_f = 30$ N · s/m has been chosen as an intermediate value between the minimum (5 N · s/m) and the maximum (60 N · s/m) values used in the experiments. The default mass value $\lambda_f = 3$ kg and the constant values $a = 1.1820$, $b = 0.60$, $c = 0.4$, $d = 20$ have been set in order to have the minimum allowed T preserving stability.

The geometric loci in the parameters space corresponding to the above choices are represented in Fig. 4. Notice that the dot-dashed line (minimum T curve) can be also taken as the frontier of the stability region in the parameter space, which, for values of the damping D lower than 10 N · s/m, is less conservative than the geometric locus of Fig. 3 (minimum constant mass curve).

A rigorous theoretical justification of the above choices is not easy, but some hints can be derived by considering the position control scheme of Fig. 5 modeling the physical interaction

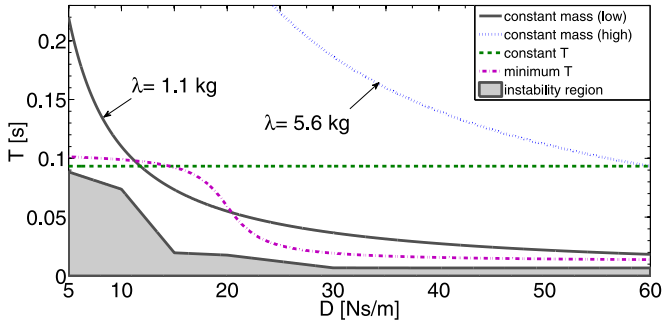

Fig. 4. Representation of the four variation laws of time constant T with respect to damping D.

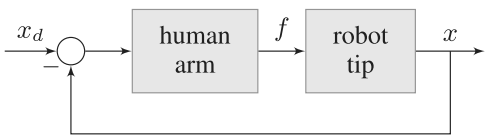

Fig. 5. Block diagram representing the human–robot physical interaction.

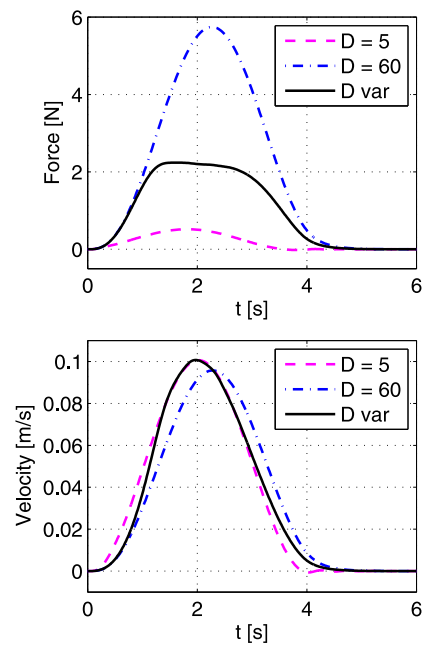

Fig. 6. Time history of the force (top) and velocity (bottom) in the case of low mass ($\lambda = 1.1$ kg) and variable damping, compared with the case of low ($D = 5\,\mathrm{N}\cdot\mathrm{s/m}$) and high ($D = 60\,\mathrm{N}\cdot\mathrm{s/m}$) constant damping.

between the human arm and the robot's tip along a single Cartesian direction. In that scheme, the human arm driving the end effector through the force f is modeled as a pure stiffness k, considering that the stiffness is the dominant effect of the impedance of the human arm (see, e.g., [7] and [8]), namely:

$$f = k(x_d - x).$$

The value $k = 200$ N/m, corresponding to an intermediate value of the arm stiffness during a writing task, has been considered in the simulations.

In view of (4), the dynamics of the end effector, in case of variable damping and mass, is represented by the nonlinear equation

$$\lambda(\dot{x})\ddot{x} + D(\dot{x})\dot{x} = f$$

where the damping D is defined in (20) and the mass λ is set constant in the cases L1 and L2 or as

$$\lambda(\dot{x}) = D(\dot{x})T$$

in the cases L3 and L4.

The position reference $x_d(t)$ is chosen according to a raised cosine time law with a duration of 4 s and a total displacement of 0.2 m.

A comparison of the performance obtained with the different choices of the parameters can be made by comparing the forces f applied by the human to the robot's tip and the resulting velocities.

In Fig. 6, the scheme with variable damping is compared with the case of constant damping set to the minimum ($D = 5\,\mathrm{N}\cdot\mathrm{s/m}$) and maximum ($D = 60\,\mathrm{N}\cdot\mathrm{s/m}$) values, respectively. It can be observed that the force required to move the end effector in the case of variable damping reaches intermediate values with respect to those required in the case of minimum and maximum constant damping. On the other hand, when the velocity is higher, the velocity profile in the case of variable damping is quite close to that obtained in the case of minimum damping. For low velocity, the profile is closer to that in the case of maximum damping.

It is worth noticing that, when constant minimum damping is used, the velocity almost matches the desired one (not reported in the figure); however, when the velocity decreases to zero, both the force and the velocity are oscillating and change sign. This undesirable behavior is emphasized when the mass is set to the maximum value, as shown in Fig. 7, but is not present in the other cases where, although the force is higher than in the case of minimum damping, both force and velocity go to zero smoothly and without oscillations.

In can be argued that, with respect to the velocity and force profiles, the use of variable damping allows to reach a good compromise with respect to the cases of constant low and high damping.

On the other hand, when variable mass is used in addition to variable damping, the simulation results show that the performance do not change significantly with respect to the case of constant mass. Slightly better results are obtained when the virtual mass is lower, i.e., in the case L4 better than in the case L3.

The suggestions deriving from the above analysis are based on simplified assumptions, one for all, the hypothesis that the stiffness of the human arm remains constant during the task execution. For this reason, the experimental validation reported in the next section is of crucial importance.

VII. Experiments

In the experiments, two fundamental aspects have been considered, namely, the use of redundancy and the choice of the variable impedance strategy.

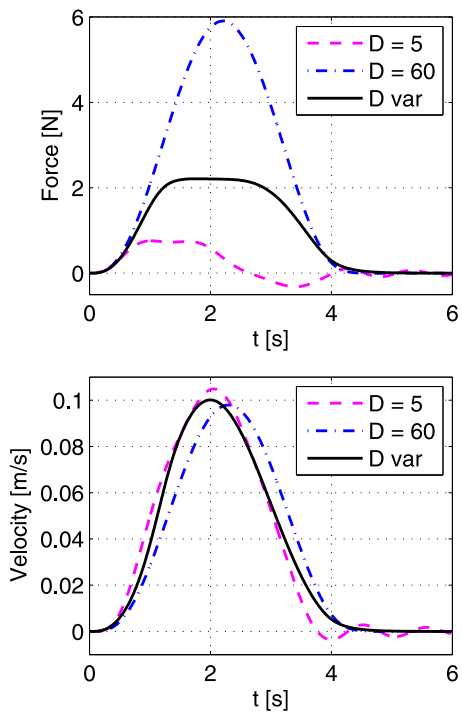

Fig. 7. Time history of the force (top) and velocity (bottom) in the case of high mass ($\lambda = 5.6$ kg) and variable damping, compared with the case of low ($D = 5\,\mathrm{N}\cdot\mathrm{s/m}$) and high ($D = 60\,\mathrm{N}\cdot\mathrm{s/m}$) constant damping.

A case study has been selected, consisting in the execution of a writing task on a horizontal plane operated by a human: the operator guides a paint marker mounted on the robot's tip along a path drawn on a paper sheet.

The orientation was not considered in our case study; otherwise, we will not have significant redundant DOFs that can be used for the secondary task. Moreover, the aim of our work is to check the value of the proposed approach for a generic task of comanipulation requiring only Cartesian position control.

The path has been designed with the aim of inducing trajectories with variable velocity and is composed of long straight-line segments, sharp corners, and smooth circular arcs (see Fig. 10, dot-dashed lines).

The initial configuration of the robot has been chosen to facilitate the execution of the writing task planned on the horizontal plane, namely

$$\boldsymbol{q}_i = [2.35 \quad 22.8 \quad -1.54 \quad -53.2 \quad -3.1 \quad 101.15 \quad 0]^T$$

with inertia matrix

$$\boldsymbol{\Lambda}(\boldsymbol{q}_i) = \begin{bmatrix} 0.1265 & -0.0042 & 0.1470 \\ -0.0042 & 0.2002 & -0.0661 \\ 0.1470 & -0.0661 & 2.9396 \end{bmatrix}$$

and eigenvalues

$$\boldsymbol{\lambda}(\boldsymbol{q}_i) = (\,0.1188 \quad 0.1986 \quad 2.9489\,)^T$$

where the joint angles are in degrees.

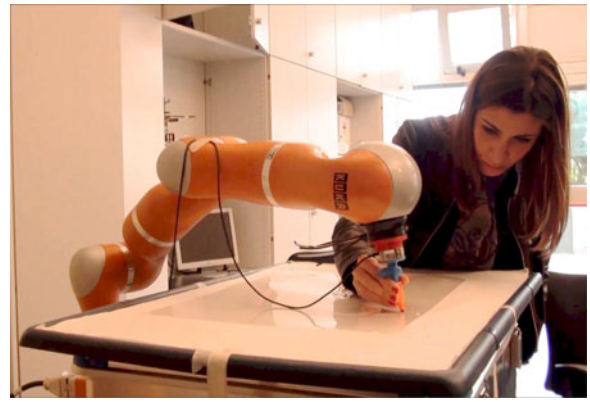

Fig. 8. Snapshot of the comanipulation task.

A. Redundancy Versus Stability

Two different secondary tasks have been tested for redundancy resolution: the maximization of the kinematic manipulability index (11) and the minimization of the DCI (14).

Here, the comparison is carried out by checking the stability of the Cartesian impedance control law, i.e., verifying that the system remains stable during task execution, when variable impedance control is applied. A snapshot of the comanipulation task is reported in Fig. 8; the complete video sequence can be found in the accompany video.

In Section V, a conservative stability region in the parameter space has been found, assuming that the same damping and mass parameters are set along all the Cartesian directions. A more accurate estimation of the stability region can be found, by using the same experimental procedure described in Section V, but allowing the choice of different values of the parameters along the three Cartesian directions.

The stability regions for the three Cartesian directions of the end effector, referred to the base frame, are shown in Fig. 9. In the same figure, two sets of curves are represented, corresponding to constant mass (or inertia) loci. The continuous curves, with constant virtual inertia $\boldsymbol{\Lambda}_d = \mathrm{diag}\{0.0328, 0.0548, 0.8138\}$ kg, are close to the instability frontiers and can be assumed as minimal inertia curves. The dashed curves, with $\boldsymbol{\Lambda}_d = \mathrm{diag}\{0.0492, 0.0822, 1.2207\}$ kg, are safely within the stability regions. The experiments have been performed using a variable damping impedance control law, with parameters varying on the above curves, namely, constant inertia and damping set according to (20).

When the DCI is used for redundancy resolution, the task has been completed in both cases, as it is shown in Fig. 10, where the paths of the paint marker are represented, together with the reference path, when low and high values of virtual inertia are used, respectively. On the other hand, in the case of low inertia (Fig. 10, top), the task cannot be completed when the manipulability index (Man) is used for redundancy resolution, because the system tends to become unstable. The accuracy of the path and the time to complete the task have not been evaluated at this stage.

The corresponding time histories of the DCI during the execution of the experiment are reported in Fig. 11. Notice that

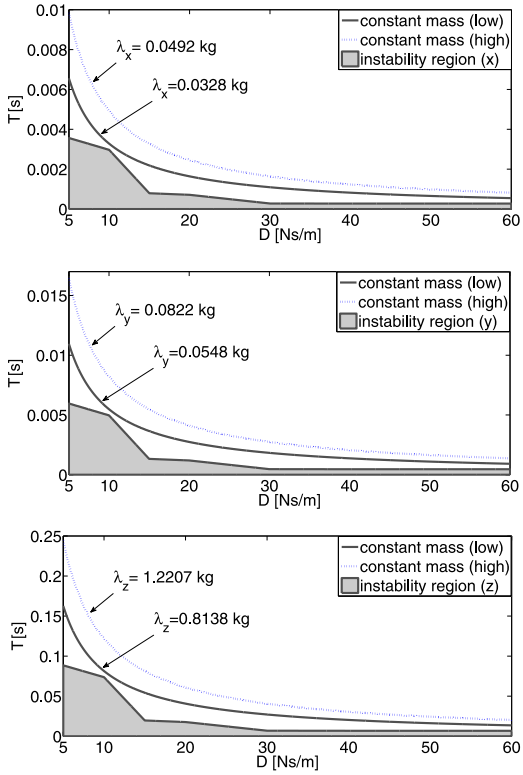

Fig. 9. Stability regions and constant mass curves for the three Cartesian directions.

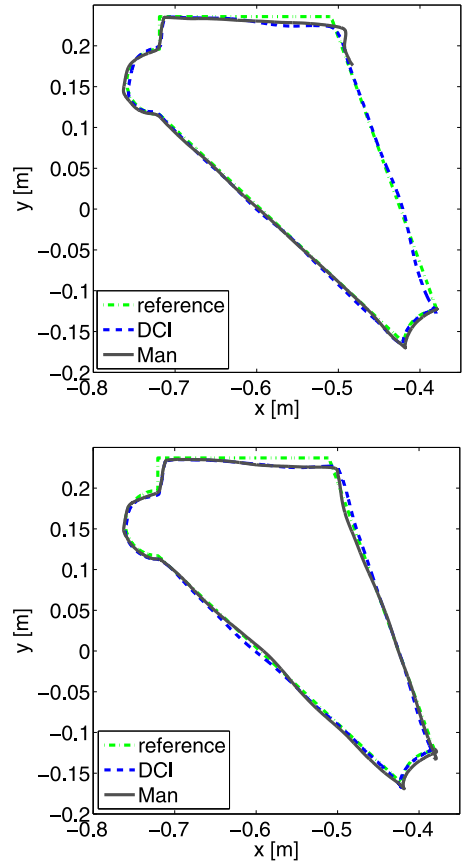

Fig. 10. Reference and actual paths for the writing task in the case of low (top) and high (bottom) virtual inertia.

the values of the DCI are always lower when the minimization of the DCI is used as secondary task, as expected, with some exceptions in correspondence of abrupt changes of directions. Moreover, in the case of low inertia, the system tends to become unstable when the value of the DCI is too high, i.e., when the inertia of the robot at the end effector deviates significantly from the desired diagonal inertia imposed by the control.

B. Redundancy Versus Performance

To evaluate the performance related to redundancy resolution, the methods have been compared using two different impedance laws, one with constant parameters (set as $\lambda = 1.1$ kg, $D = 60$ N $\cdot$ s/m) and one with variable damping (low constant mass, $\lambda = 1.1$ kg, of Fig. 4).

Since the objective is to compare the redundancy resolution strategies, a generic choice for the impedance parameters is made by setting them uniformly in all the directions. Moreover, as described in the previous Section VII-A, when redundancy is used to optimize the manipulability, a more conservative choice for the impedance parameters is needed, since the stability limits in the three Cartesian directions found experimentally in the neighborhood of the initial configuration (see Fig. 6) are not satisfied throughout the drawn path.

Since the assigned task consists in pursuing a given path, a significant measure of performance is the error between the reference and the actual path, which can be defined in different ways. A very simple measure is the absolute value of the differ-

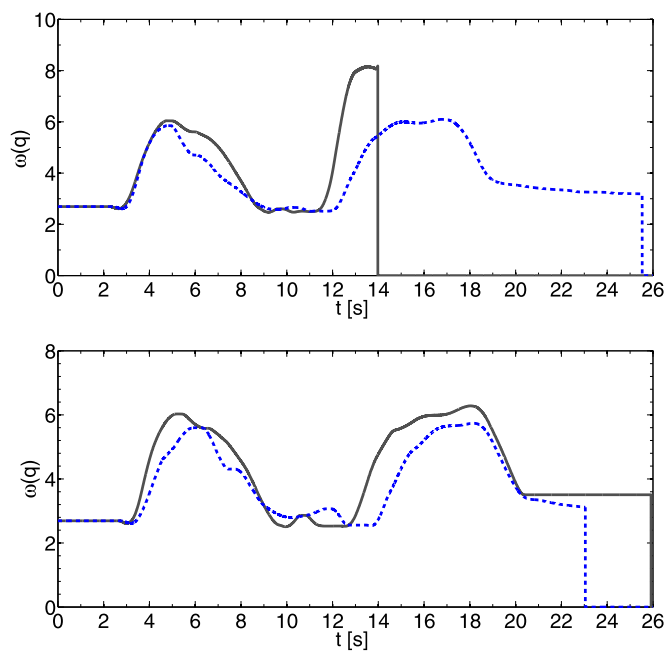

Fig. 11. Time histories of the values of DCI in the case of low (top) and high (bottom) virtual inertia. The continuous lines represent the DCI when redundancy is used to increase manipulability. The dashed lines represent the DCI when redundancy is used to minimize the DCI.

TABLE I
t-TEST RESULTS ON THE DATA OF FIG. 15

	var vr hconst	var vr lconst	hconst vr lconst
time	$h = 1$ var< hconst ($p = 0.0062$)	$h = 0$ – ($p = 0.8888$)	$h = 0$ – ($p = 0.4503$)
length	$h = 0$ – ($p = 0.9739$)	$h = 1$ var< lconst ($p = 0.0094$)	$h = 1$ hconst< lconst ($p = 0.0313$)

ence between the length of the path drawn in cooperation with the robot, l_e, and the ideal path length, l_d, namely the length error

$$e = |l_d - l_e|. \tag{21}$$

We have also tested more accurate measures, as the area of the region between the ideal and the actual path, or the difference between the centroid of the reference and actual figure. For the purpose of our experiments, however, the measure (21) provided satisfactory results.

Another performance parameter is the execution time H of the trajectory, defined as the difference between the time when the entire path is completed and the time when the drawing tool touches the paper on the desk to start writing.

In order to obtain quantities that overcome the skills of the singular operator, the above parameters are evaluated as the average on the performance of more subjects.

The tests have been carried out on five different subjects that move the robot using their dominant hand. We found that the number of subjects used in the experiments is sufficient on the basis of the analysis of the results. Indeed, the results of the comparison between the variable and constant (low and high) impedance are statistically significant as shown in Table I reported at the end of this section.

Each subject has been trained in advance, by executing the task with the different strategies to be tested, in order to become familiar with the task and the robot. At the end of the training phase, all the subjects were able to complete the task in a reasonable time (under 30 s) with all the control strategies. In addition, during the training phase, each subject was asked to look for the configuration, which resulted the most comfortable, as well as for the best fitting starting point of the path, without any kind of conditioning.

The subjects were told to perform the path taking into account the accuracy as a primary objective and the execution time as a secondary objective. In addition, during both the training phase and the actual testing phase, the subjects have not been informed on the features of each control law, nor even which one of the four strategies they were performing.

The results of the tests are reported in Fig. 12, where the error on the length of the path e versus the execution time H is reported for all the subjects, as well as their mean values.

It can be observed that, for the impedance control with constant parameters, the use of DCI ensures better performance than the use of manipulability index (Man) both in terms of execution time and error on the path. This is true also for variable impedance control even though the use of variable parameters reduces the error on the path in spite of the strategy used to solve the redundancy.

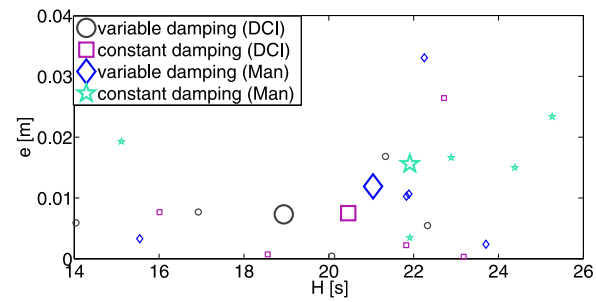

Fig. 12. Values of the length error e and execution time H in the experiments on five subjects using variable and low constant impedance; both manipulability index and DCI optimization are used as secondary tasks. The bigger markers are the mean values on the five different subjects.

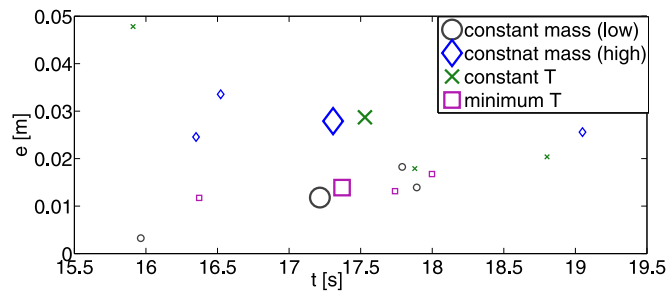

Fig. 13. Values of length error e and execution time H in the experiments on three subjects using DCI optimization and the four variable impedance laws of Fig. 4. The bigger markers are the mean values on the three different subjects.

Last but not least, all the subjects involved in the experiments have confirmed that the "feeling" of the manual guidance (in terms of intuitiveness and response of the robot) improves when the DCI is adopted, i.e., when redundancy is used to decouple the natural end effector dynamics along the principal directions of the task.

C. Evaluation of Variable Impedance Laws

In this set of experiments, the DCI is adopted for redundancy resolution, and the performance of the different variable impedance laws, presented in Section VI, is evaluated. The same task described in the previous sections has been executed by three different subjects.

The results, reported in Fig. 13, show that the lower error along the path with the smaller execution time is achieved when the virtual mass of the end effector is kept constant, to the minimum value compatible with stability, namely, the law L1 (see also Fig. 4).

D. Variable Versus Constant Impedance

The variable impedance control L1 has been compared with two different sets of constant impedance gains (chosen along the curve), namely: high damping ($\lambda = 1.1$ kg, $D = 60$ N · s/m) and low damping ($\lambda = 1.1$ kg, $D = 20$ N · s/m). These values

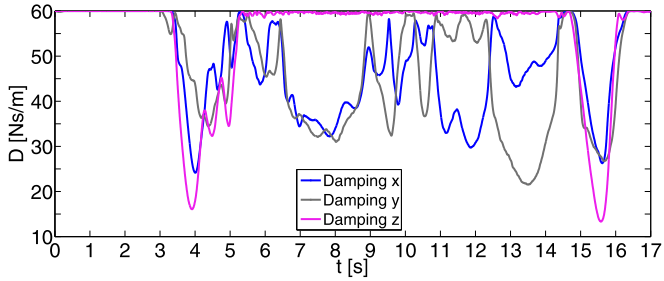

Fig. 14. Time history of the variable damping D during the execution of the task with the variable impedance control L1 for one subject.

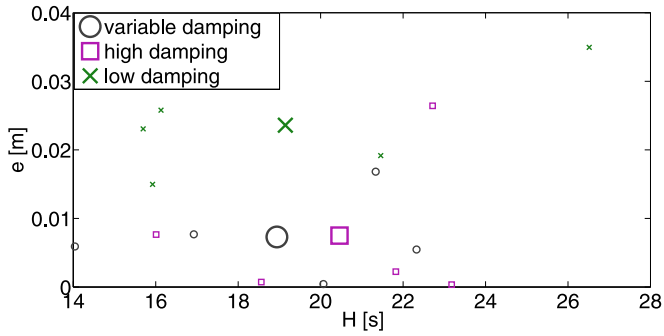

Fig. 15. Values of length error e and execution time H in the experiments on five subjects using DCI optimization, with the variable impedance control L1 and two different sets of constant parameters. The bigger markers are the mean values on the five different subjects.

correspond to the average maximum and minimum damping recorded in the previous set of experiments with constant mass and variable damping.

The time history of the damping variation along the three Cartesian directions for a single test is reported in Fig. 14. The aim of this test is that of evaluating what is resulted as the best variable impedance control law for the considered task, with two different choices of constant damping values: high damping (to privilege accuracy) and low damping (to privilege execution speed).

The results, carried out on five different subjects, are shown in Fig. 15, where the execution time H and the error on the length of the path are reported. In order to assess whether the difference between the mean values on the set of data reported in Fig. 15 is statistically significant, a t-test has been performed [36]. The results, reported in Table I, can be interpreted as follows. If the variable h is 1 (0), then the two compared means are (not) significantly different with confidence $p \in [0, 1]$; the lower the value of p, the more statistically significant the difference between the mean values of the two sets of data. Moreover, Fig. 16 represents the norm of the linear forces exerted at the tip, for one subject, in the case of high, low and variable impedance. The horizontal dashed lines are the corresponding mean values computed during the execution of the task.

Looking at Table I, the constant impedance with high damping (hconst) ensures higher accuracy with respect to the constant impedance with low damping (lconst), as expected. This result, however, comes at the expenses of the execution time and of

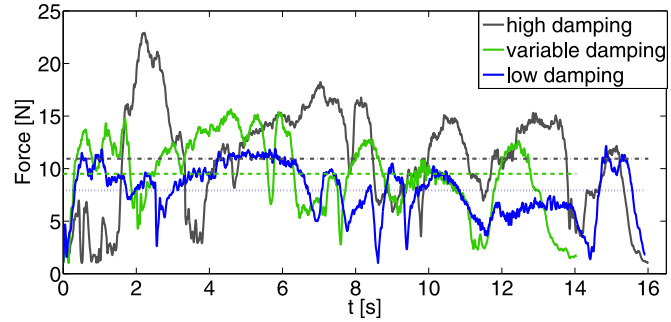

Fig. 16. Norm and mean value of the contact forces for high, variable, and low damping, for one subject.

the operator effort requested for the manual guidance. Indeed, from Fig. 16, it can be verified that higher damping requires higher forces to be exerted to the end effector. On the contrary, impedance with low damping allows the task to be performed more easily, with less effort and time, but with less accuracy.

The most relevant result of Table I is that the variable impedance (var) guarantees the best performance for accuracy, execution time, and effort of the operator (see also Figs. 15 and 16). Indeed, it can be seen that the improvement of variable impedance (var) with respect to high constant damping (hconst) in terms of execution time is statistically significant; on the contrary, it is not possible to detect an edge over the accuracy. From the comparison between the low constant damping (lconst) and variable impedance parameters (var), it emerges that the advantage of the variable strategy is relevant and statistically significant in terms of accuracy, while the difference in terms of execution time is irrelevant.

For the sake of completeness, the results of the comparison between high and low constant damping parameters have also been reported. By observing Fig. 15 and Table I, the advantage of using high damping parameters for accuracy appears clear and statistically significant. The execution time improves when low damping is adopted since the robot become lighter and easier to move (see Fig. 16). However, the result on the execution time is not statistically significant: This is probably because the subjects were instructed to prefer accuracy over speed during the execution of the task, which has led to a higher dispersion of the data related to execution time.

VIII. Discussion

During physical human–robot interaction, the most natural way to control the robot is through an impedance strategy tuned to the task requirements. Redundancy can be exploited as well to improve stability and performance. The research presented in this study branches off along these two complementary lines, both pointing toward the improvement of the physical human–robot interaction in terms of intuitiveness and stability during the execution of comanipulation tasks.

In the first instance, different strategies to solve redundancy are evaluated among the solutions that are compatible with the main task. The comparison has been made in terms of stability and performance (i.e., length error e and execution time H). The

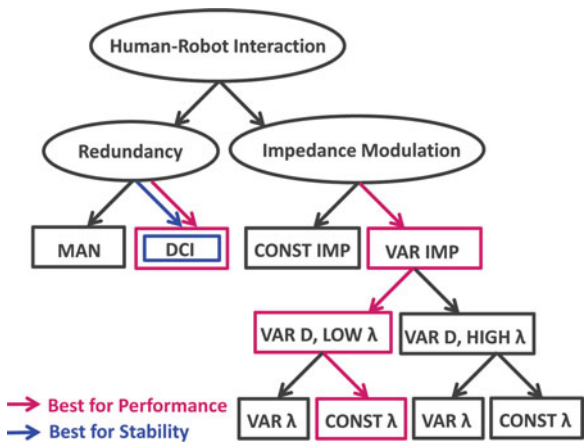

Fig. 17. Conceptual path followed for the experimental investigations. The solutions with the best results in terms of performance (i.e., length error e and execution time H) and stability are highlighted using different colours.

Fig. 18. Results obtained with different combination of redundancy resolution and impedance strategies presented on the basis of the performance level in increasing order from left to right.

experiments showed that the best way to solve redundancy in comanipulation tasks is that of keeping the end effector apparent inertia as close as possible to that imposed by the impedance control, i.e., at least diagonal. This allows a wider range of selection of the impedance parameters that preserve stability and improves the performance (see Sections VII-A and VII-B).

In parallel, the experimental evaluation of different modulation strategies of the impedance parameters has been carried out. The best solution for a lightweight robot consists on linking the damping variation directly to the Cartesian velocity, as previously discussed. The performance is improved when the virtual equivalent mass at the end effector is kept as low as possible, compatibly with the stability (see Fig. 13).

In Fig. 17, a graphical representation of the conceptual path followed in our investigation is reported. It can be seen that the best solution in terms of stability and performance is that achieved using variable damping and constant virtual mass, set to the minimum value compatible with the stability. The comparison between variable and constant impedance using different redundancy resolution strategies is summarized in Fig. 18. It can be seen that the performance improves from left to right.

A number of issues remain open. First of all, we have adopted a damping variation law (20) that is the result of an extensive experimental campaign. In the experiments, we have also tested the adaptation law presented in [15], where the damping is varied according to the acceleration, with worse results, because the system was too responsive. The modulation of the damping based on acceleration can be interpreted as a nonlinear lead compensation based on the intention of the user to increase or decrease the velocity, which enhances the reactivity of the system, resulting in a higher equivalent bandwidth. This may explain why this kind of modulation is effective on the robotic platform used in [15], based on a heavy industrial robot with moving masses ranging from 100 to 500 kg and low equivalent bandwidth, and not helpful in our platform, based on a lightweight KUKA robot with a larger equivalent bandwidth, where it causes an overreaction. In any case, a theoretical analysis supporting the choice of the modulation laws of the impedance parameters, which takes into account the nonlinear and coupled dynamics of robot and human arm, is still missing.

Another important issue is that our study does not include a rigorous stability proof, for both fixed and variable impedance parameters. As a matter of fact, although the experimental results provide significant and useful guidelines, these cannot be easily generalized to any kind of robot and task.

IX. Conclusion

In this paper, the problem of Cartesian impedance control of a redundant robot arm executing a cooperative task with a human has been addressed. In particular, redundancy has been used to keep robot's natural behavior as close as possible to the desired impedance behavior, by decoupling the end effector equivalent inertia. This allows easily finding a region in the impedance parameter space where stability is preserved. Extensive experimental tests confirmed that this solution leads to improving performance in the execution of a cooperative writing task with respect to the use of other options for redundancy resolution, e.g., the maximization of the manipulability index.

Moreover, different variable impedance strategies, where the parameters are modified on the basis of the interpretation of human intentions, have been evaluated in a simulation study and tested on the experimental setup. The variable impedance strategy ensuring the best performance has been selected and compared with two different sets of constant impedance gains, i.e., high damping (to privilege accuracy) and low damping (to privilege execution speed).

The experimental results show that the combination of variable impedance and redundancy resolution with inertia decoupling ensures the best tradeoff between accuracy and execution time.

References

[1] N. Hogan, "Impedance control: An approach to manipulation: Part I theory; Part II implementation; Part III applications," *J. Dyn. Sys., Meas., Control*, vol. 107, no. 12, pp. 1–24, 1985.

[2] H. Sadeghian, L. Villani, M. Keshmiri, and B. Siciliano, "Task-space control of robot manipulators with null-space compliance," *IEEE Trans. Robot.*, vol. 30, no. 2, pp. 493–506, Apr. 2014.

[3] F. Ficuciello, A. Romano, L. Villani, and B. Siciliano, "Cartesian impedance control of redundant manipulators for human-robot comanipulation," in *Proc. IEEE/RSJ Int. Conf. Intell. Robots Syst.*, Chicago, IL, USA, 2014, pp. 2120–2125.

[4] B. Vanderborght, A. Albu-Schaeffer, A. Bicchi, E. Burdet, D. Caldwell, R. Carloni, M. Catalano, O. Eiberger, W. Friedl, G. Ganesh, M. Garabini, M. Grebenstein, G. Grioli, S. Haddadin, H. Hoppner, A. Jafari, M.

Laffranchi, D. Lefeber, F. Petit, S. Stramigioli, N. Tsagarakis, M. V. Damme, R. V. Ham, L. Visser, and S. Wolf, "Variable impedance actuators: A review," *Robot. Auton. Syst.*, vol. 61, no. 12, pp. 1601–1614, 2013.

[5] R. Ikeura and H. Inooka, "Variable impedance control of a robot for cooperation with a human," in *Proc. IEEE Int. Conf. Robot. Autom.*, Nagoya, Aichi, Japan, 1995, pp. 3097–3102.

[6] R. Ikeura, T. Moriguchi, and K. Mizutani, "Optimal variable impedance control for a robot and its application to lifting an object with a human," in *Proc. IEEE Int. Workshop Robot Human Interactive Commun.*, Berlin, Germany, 2002, pp. 500–505.

[7] T. Tsumugiwa, R. Yokogawa, and K. Hara, "Variable impedance control based on estimation of human arm stiffness for human-robot cooperative calligraphic task," in *Proc. IEEE Int. Conf. Robot. Autom.*, Washington, DC, USA, 2002, pp. 644–650.

[8] C. Mitsantisuk, K. Ohishi, and S. Katsura, "Variable mechanical stiffness control based on human stiffness estimation," in *Proc. IEEE Int. Conf. Mechatronics*, Istanbul, Turkey, 2011, pp. 731–736.

[9] K. P. Tee, D. W. Franklin, M. Kawato, T. T. Milner, and E. Burdet, "Concurrent adaptation of force and impedance in the redundant muscle system," *Biol. Cybern.*, vol. 102, no. 1, pp. 31–44, 2010.

[10] E. Burdet, R. Osu, D. Franklin, T. E. Milner, and M. Kawato, "The central nervous system stabilizes unstable dynamics by learning optimal impedance," *Nature*, vol. 414, no. 6862, pp. 446–449, 2001.

[11] C. Yang, G. Ganesh, S. Haddadin, S. Parusel, A. Albu-Schaeffer, and E. Burdet, "Human-like adaptation of force and impedance in stable and unstable interactions," *IEEE Trans. Robot.*, vol. 27, no. 5, pp. 918–930, Apr. 2011.

[12] M. Howard, D. Braun, and S. Vijayakumar, "Transferring human impedance behavior to heterogeneous variable impedance actuators," *IEEE Trans. Robot.*, vol. 29, no. 4, pp. 847–862, Aug. 2013.

[13] K. Kronander and A. Billard, "Online learning of varying stiffness through physical human-robot interaction," in *Proc. IEEE Int. Conf. Robot. Autom.*, St. Paul, MN, USA, 2012, pp. 1842–1849.

[14] A. Ajoudani, N. Tsagarakis, and A. Bicchi, "Tele-impedance: Teleoperation with impedance regulation using a body-machine interface," *Int. J. Robot. Res.*, vol. 31, no. 13, pp. 1642–1656, 2012.

[15] A. Lecours, B. Mayer-St-Onge, and C. Gosselin, "Variable admittance control of a four-degree-of-freedom intelligent assist device," in *Proc. IEEE Int. Conf. Robot. Autom.*, Saint Paul, MN, USA, 2012, pp. 3903–3908.

[16] F. Ferraguti, C. Secchi, and C. Fantuzzi, "A tank-based approach to impedance control with variable stiffness," in *Proc. IEEE Int. Conf. Robot. Autom.*, Karlsruhe, Germany, 2014, pp. 4933–4938.

[17] S. Bowyer, B. Davies, and F. R. y Baena, "Active constraints/virtual fixtures: A survey," *IEEE Trans. Robot.*, vol. 30, no. 1, pp. 138–157, Feb. 2014.

[18] C. A. Moore, M. A. Peshkin, and J. E. Colgate, "Cobot implementation of virtual paths and 3-d virtual surfaces," *IEEE Trans. Robot.*, vol. 19, no. 2, pp. 347–351, Apr. 2003.

[19] V. Duchaine, B. Mayer-St-Onge, D. Gao, and C. Gosselin, "Stable and intuitive control of an intelligent assist device," *IEEE Trans. Haptics*, vol. 5, no. 2, pp. 1939–1412, Apr–Jun. 2012.

[20] S. Buerger and N. Hogan, "Complementary stability and loop shaping for improved human-robot interaction," *IEEE Trans. Robot.*, vol. 23, no. 2, pp. 232–244, Apr. 2007.

[21] J. Colgate and H. Hogan, "Robust control of dynamically interacting systems," *Int. J. Control*, vol. 48, no. 1, pp. 65–88, 1988.

[22] W. Newman, "Stability and performance limits of interaction controllers," *ASME J. Dyn. Syst., Meas. Control*, vol. 114, no. 4, pp. 563–570, 1992.

[23] S. Buerger and N. Hogan, "Relaxing passivity for human-robot interaction," in *Proc. IEEE/RSJ Int. Conf. Intelli. Robots Syst.*, Beijing, China, 2006, pp. 4570–4575.

[24] V. Duchaine and C. Gosselin, "Investigation of human-robot interaction stability using Lyapunov theory," in *Proc. IEEE Int. Conf. Robot. Autom.*, Pasadena, CA, USA, 2008, pp. 2189–2194.

[25] C. Ott, R. Mukherjee, and Y. Nakamura, "Unified impedance and admittance control," in *Proc. IEEE Int. Conf. Robot. Autom.*, Anchorage, AK, USA, 2010, pp. 554–561.

[26] O. Khatib, "A unified approach for motion and force control of robot manipulators: The operational space formulation," *IEEE J. Robot. Autom.*, vol. 3, no. 1, pp. 1115–1120, Feb. 1987.

[27] Y. Nakamura and H. Hanafusa, "Inverse kinematic solution with singularity robustness for robot manipulator control," *ASME J. Dyn. Syst., Meas. Control*, vol. 108, pp. 163–171, 1986.

[28] C. Ott, *Cartesian Impedance Control of Redundant and Flexible Joint Robots* (Springer Tracts in Advanced Robotics), vol. 49. New York, NY, USA: Springer, 2008.

[29] A. D. Luca, A. Albu-Schäffer, S. Haddadin, and G. Hirzinger, "Collision detection and safe reaction with the DLR-III lightweight robot arm," in *Proc. IEEE/RSJ Int. Conf. Intell. Robots Syst.*, Beijing, China, 2006, pp. 1623–1630.

[30] J. Nakanishi, R. Cory, M. J. Peters, and S. Schaal, "Operational space control: A theoretical and empirical comparison," *Int. J. Robot. Res.*, vol. 27, no. 6, pp. 737–757, 2008.

[31] C. Natale, B. Siciliano, and L. Villani, "Spatial impedance control of redundant manipulators," in *Proc. IEEE Int. Conf. Robot. Autom.*, Detroit, MI, USA, 1999, pp. 1788–1793.

[32] H. Sadeghian, L. Villani, M. Keshmiri, and B. Siciliano, "Dynamic multi-priority control in redundant robotic systems," *Robotica*, vol. 31, no. 7, pp. 1155–1167, 2013.

[33] C. Dietrich, C. Ott, and A. Albu-Schäffer, "Multi-objective compliance control of redundant manipulators: Hierarchy, control, and stability," in *Proc. IEEE/RSJ Int. Conf. Intell. Robots Syst.*, Tokyo, Japan, 2013, pp. 3043–3050.

[34] J. Park, W. Chung, and Y. Youm, "Computation of gradient of manipulability for kinematically redundant manipulators including dual manipulators system," *Trans. Control Autom. Syst. Eng.*, vol. 1, no. 1, pp. 8–15, 1999.

[35] O. Ma and J. Angeles, "The concept of dynamic isotropy and its applications to inverse kinematics and trajectory planning," in *Proc. IEEE Int. Conf. Robot. Autom.*, San Francisco, CA, USA, 1990, pp. 10–15.

[36] M. Hazewinkel, Ed.,*Encyclopedia of Mathematics*. New York, USA: Springer-Verlag, 2001.

Fanny Ficuciello (M'11) was born in Nocera Inferiore, Italy, on October 20, 1974. She received the Laurea degree (*magna cum laude*) in mechanical engineering in 2007 and the Ph.D. degree in computer and automation engineering from University of Naples Federico II, Napoli, Italy, in November 2010.

From September to March 2010 she was a Visiting Scholar with the Control Engineering Group, University of Twente, Enschede, The Netherlands, under the supervision of Prof. S. Stramigioli. She is a Member of PRISMA (Projects of Industrial and Service Robotics, Mechatronics and Automation) Research Group. She is currently a Postdoctoral Researcher with University of Naples Fedeerico II. Her research interest is focused on robotics, in particular on safe physical human–robot interaction, force/impedance control, grasping, and manipulation control of anthropomorphic hand-arm systems. She has published more than 20 journal and conference papers and book chapters.

Luigi Villani (S'94–M'97–SM'03) was born in Avellino, Italy, on December 5, 1966. He received the Laurea degree in electronic engineering and the Research Doctorate degree in electronic engineering and computer science from University of Naples, Naples, Italy, in 1992 and 1996, respectively.

He is an Associate Professor of automatic control with the Department of Electrical Engineering and Information Technology, University of Naples. He has coauthored six books and more than 50 journal papers and 100 conference papers and book chapters. His book *Robotics: Modelling, Planning and Control* is one of the most widely adopted textbooks worldwide. His research interests include force/motion control of manipulators, safe physical human–robot interaction, cooperative robot manipulation, lightweight flexible arms, adaptive and nonlinear control of mechanical systems, visual servoing, fault diagnosis, and fault tolerance for dynamical systems.

Dr. Villani was an Associate Editor of IEEE TRANSACTIONS ON ROBOTICS from 2007 to 2011 and Associate Editor of IEEE TRANSACTIONS ON CONTROL SYSTEMS TECHNOLOGY from 2005 to 2012.

Bruno Siciliano (M'91–SM'94–F'00) was born in Naples, Italy, on October 27, 1959. He received the Laurea degree and the Research Doctorate degree in electronic engineering from University of Naples, Naples, in 1982 and 1987, respectively.

He is currently a Professor of control and robotics and the Director of the PRISMA (Projects of Industrial and Service Robotics, Mechatronics and Automation) Laboratory, Department of Electrical Engineering and Information Technology, University of Naples. He has coauthored seven books, 80 journal papers, and 230 international conference papers and book chapters. His book *Robotics: Modelling, Planning and Control* is one of the most widely adopted textbooks worldwide. He has delivered 140 invited lectures and seminars at institutions worldwide. His research interests include identification and adaptive control, impedance and force control, visual tracking and servoing, redundant and cooperative manipulators, lightweight flexible arms, aerial robots, and human-centered and service robotics.

Dr. Siciliano is a Fellow of the American Society of Mechanical Engineers and the International Federation of Automatic Control. He is Co-Editor of *Springer Tracts in Advanced Robotics* series, and has served on the Editorial Boards of several journals as well as Chair or Co-Chair for numerous international conferences. He co-edited the *Springer Handbook of Robotics*, which received the AAP PROSE Award for Excellence in Physical Sciences and Mathematics and was also the winner in the category Engineering and Technology. His group has been granted 14 European projects, including an Advanced Grant from the European Research Council. He has served the IEEE Robotics and Automation Society as President, as Vice President for Technical Activities and Vice President for Publications, as a member of the AdCom, and as a Distinguished Lecturer. He has received several awards, including the 2015 IEEE RAS George Saridis Leadership Award in Robotics and Automation.